The Astrophysical Journal, 819:50 (7pp), 2016 March 1 doi:10.3847/0004-637X/819/1/50

THE ABELL 85 BCG: A NUCLEATED, CORELESS GALAXY

Juan P. Madrid[1,2] and Carlos J. Donzelli[3,4]
[1] Gemini Observatory, Southern Operations Center, Colina El Pino s/n, La Serena, Chile
[2] CSIRO, Astronomy and Space Science, P.O. Box 76, Epping, NSW 1710, Australia
[3] Instituto de Astronomía Teórica y Experimental, CONICET-UNC, Laprida 922, Córdoba, Argentina
[4] Observatorio Astronómico de Córdoba, UNC, Laprida 854, Córdoba, Argentina
Received 2015 July 12; accepted 2016 January 5; published 2016 February 26

ABSTRACT

New high-resolution *r*-band imaging of the brightest cluster galaxy (BCG) in Abell 85 (Holm 15A) was obtained using the Gemini Multi Object Spectrograph. These data were taken with the aim of deriving an accurate surface brightness profile of the BCG of Abell 85, in particular, its central region. The new Gemini data show clear evidence of a previously unreported nuclear emission that is evident as a distinct light excess in the central kiloparsec of the surface brightness profile. We find that the light profile is never flat nor does it present a downward trend toward the center of the galaxy. That is, the new Gemini data show a different physical reality from the featureless, "evacuated core" recently claimed for the Abell 85 BCG. After trying different models, we find that the surface brightness profile of the BCG of Abell 85 is best fit by a double Sérsic model.

Key words: galaxies: clusters: general – galaxies: individual (Abell 85, Holm 15A) – galaxies: nuclei – galaxies: structure

1. INTRODUCTION

Within the current framework of hierarchical structure formation (e.g., White & Rees 1978) galaxy clusters are formed through the successive mergers of galaxies, galaxy groups, and subclusters. Thus, galaxy clusters form the largest gravitationnally bound structures in the universe. Interestingly, X-ray observations have shown that most of the baryonic mass of galaxy clusters resides not in galaxies but in their hot intracluster gas (e.g., Jones & Forman 1984).

Abell 85 is a rich galaxy cluster located at a redshift of $z \sim 0.0555$ with 305 confirmed cluster members (Durret et al. 1998). Abell 85 is a bright X-ray source that has been extensively studied using several X-ray satellites (e.g., Markevitch et al. 1998; Lima Neto et al. 2001; Sivakoff et al. 2008). The X-ray emission of Abell 85 testifies to an intense past merging activity (Durret et al. 2005). Moreover, Abell 85 is not fully relaxed and is currently merging with at least two satellite subclusters (Kempner et al. 2002). The complex dynamical state of Abell 85 was recently discussed in great detail by Ichinohe et al. (2005). Due to its richness, Abell 85 has also been the target of several studies on the morphology–density relation (e.g., Fogarty et al. 2014).

Located in the core of galaxy clusters, and formed through a rich merger history, brightest cluster galaxies are, in turn, the most massive and luminous galaxies in the universe (De Lucia & Blaizot 2007). Recently, López-Cruz et al. (2014) reported that the brightest cluster galaxy (BCG) of Abell 85 has the largest galaxy core ever discovered. Note that the BCG of Abell 85 has also been identified as Holm 15A. The unusually large core in the surface brightness profile of the Abell 85 BCG translates into the presence of a supermassive black hole with masses above $M_\bullet \sim 10^{11} M_\odot$. The mass of the black hole is obtained by using scaling relations between galaxy cores and black hole masses (e.g., Kormendy & Ho 2013).

The results of López-Cruz et al. (2014) were challenged by Bonfini et al. (2015) who find that the Abell 85 BCG does not have a depleted core. In fact, Bonfini et al. (2015) find that a Sérsic profile plus an outer exponential component provide a good fit to the data.

Galaxy cores are defined as a relative light deficit toward the nucleus of the galaxy compared to the inward extrapolation of the surface brightness profile of the outer components of the galaxy. The physical theory postulated to explain the presence of these cores is the action of binary supermassive black holes that, through three-body interactions, slingshot away stars in the galactic center (Begelman et al. 1980).

Due to their possible link to black holes and galaxy formation, the study of cores is an active field with many authors looking at different theoretical and observational aspects. For instance, through *N*-body simulations, Milosavljević & Merritt (2001) modeled the decay of a black hole binary and how it carves galactic cores. Observationally, a major development in the study of galaxy cores came with the analysis of Advanced Camera for Surveys (ACS) data. This instrument on board the *Hubble Space Telescope* (*HST*) provided both superb resolution and large radial coverage, key factors in deriving an accurate surface brightness profile. Ferrarese et al. (2006) use a uniform sample of 100 galaxies in Virgo imaged with the ACS to derive their surface brightness profile. They find that the surface brightness profiles of most galaxies are well fit by a Sérsic (1968) profile. Earlier studies of galaxy cores with the *HST* include the work of Faber et al. (1997) and Laine et al. (2003), among many others.

In the following sections, we present high-resolution Gemini observations that have been obtained in order to study in detail the surface brightness profile of the Abell 85 BCG, particularly focusing on its nuclear region.

2. GEMINI OBSERVATIONS OF ABELL 85

Gemini South observations of Abell 85 were obtained under the Director's Discretionary Time program GS-2014B-DD-6. Abell 85 was observed with the Gemini Multi Object Spectrograph (GMOS) on imaging mode with the detector centered on the BCG, as shown in Figure 1. The data was

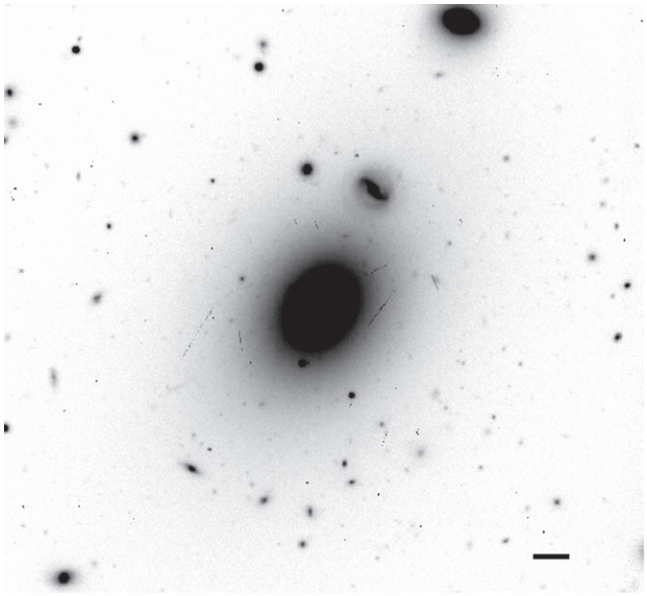

Figure 1. Gemini Multi Object Spectrograph image of Abell 85. The scale bar on the lower right represents a length of 10 kpc. North is up and east is left.

obtained on 2014 November 15 under stable atmospheric conditions on Cerro Pachón with a seeing of 0.56 arcsec.

Two exposures of 200 s each were acquired during that night. The filter in use was *r_G*0326, this filter is centered at 630 nm and has a filter width of 136 nm. We used a 2×2 binning that gives an effective pixel scale of 0.160 arcsec per pixel.

We adopt a redshift of Abell 85 $z \sim 0.0555$ which yields a distance of 233.9 Mpc and a scale of 1.075 kpc/arcsec. The Gemini-GMOS pixel scale for this observation of Abell 85 is thus 172 pc/pixel.

3. DATA REDUCTION AND ANALYSIS

Data were processed with the standard Gemini PyRAF package using the tasks described in this section. We obtained bias and twilight flats from the observatory. These calibration files were already processed through the tasks GBIAS and GIFLAT. The science images were bias subtracted and divided by the flatfield using the task GIREDUCE. These data were acquired using the new CCD detectors (Hamamatsu) recently installed on GMOS. Raw science data files have 12 extensions reflecting the fact that the detector has three CCDs and four amplifiers per CCD. A single component image was made for each of the two exposures using the task GMOSAIC. The final science image was created combining the two exposures using the task IMCOADD.

For the study of the surface brightness profile, the task LUCY, within STSDAS, is used to deconvolve the image by applying the Lucy–Richardson algorithm (Richardson 1972; Lucy 1974). The task LUCY converges after nine iterations yielding a final resolution of 0.″45.

The ELLIPSE routine (Jedrzejewski 1987) is applied to the science image in order to extract the 1D luminosity profile of the Abell 85 BCG. This profile, directly obtained from the science image is shown in Figure 2 as blue circles.

In order to obtain an accurate light profile for the targeted galaxy, all nearby sources are properly masked and the task ELLIPSE is ran iteratively until the surface brightness profile converges. We also ran the task ELLIPSE with different initial parameters, while we held some (or all) of the parameters (center, position angle, and ellipticity) fixed to a constant value to test whether we observe possible variations of the luminosity profile. The resulting luminosity profile turned out to be robust and shows no dependence on the initial parameters. Also, we did not observe any shift in the center of the isophotes during this experiment. Ellipticity remained mainly constant i.e., $0.05 < e < 0.1$. within the innermost few arcseconds. Small ellipticity values imply relatively large errors for the position angle.

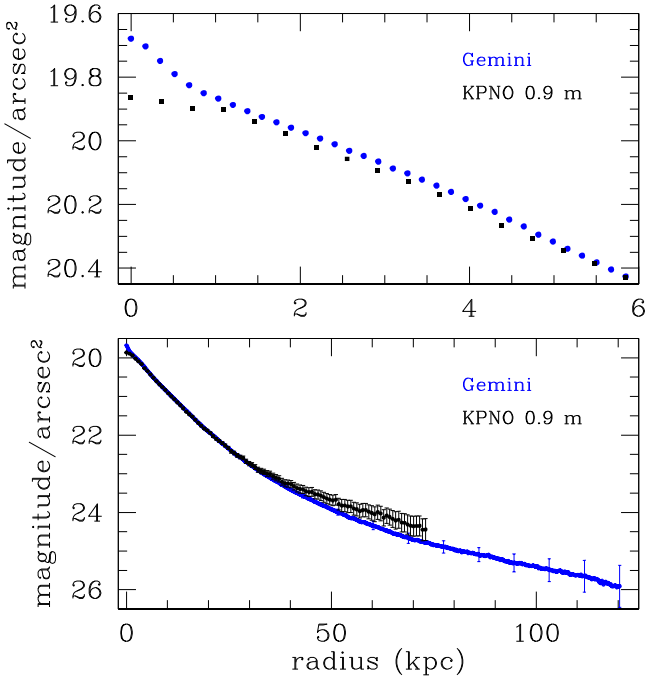

Figure 2. Surface brightness profile of the Abell 85 BCG based on our new Gemini data and the KPNO 0.9 m data published by López-Cruz et al. (2014). Top panel: zoom of the inner 6 kpc. The new Gemini data show nuclear emission not present in the KPNO 0.9 m data analyzed by López-Cruz et al. (2014). Bottom panel: Gemini and KPNO 0.9 m data up to 120 kpc in radius. The surface brightness profile of the KPNO data becomes noisy beyond ~40 kpc. Our new Gemini data goes two magnitudes fainter than the KPNO data before reaching similar noise levels.

Appropriately removing the sky background is also of great importance in order to obtain an accurate surface brightness profile. The GMOS imager provides a relatively large field of view, at least when compared to *HST* detectors, this allows us to make a first estimate of the sky background in an area of the detector where the Abell 85 BCG has very low emission.

Data taken by the Canada–France–Hawaii-Telescope (CFHT) and the surface brightness profile of this galaxy published by Donzelli et al. (2011) were also used to estimate the sky background. CFHT data of Abell 85, in the *r* band, taken under the Multi-Epoch Nearby Cluster Survey (MENeaCS; Sand et al. 2011) in 2008 September. The basic assumption we use is that the surface brightness profile of the BCG of Abell 85 should be identical at intermediate radii, independent of the telescope in use.

Once a correct estimate of the background is made, both Gemini and CFHT surface brightness profiles agree well, with the exception of the galaxy core where seeing effects dominate.

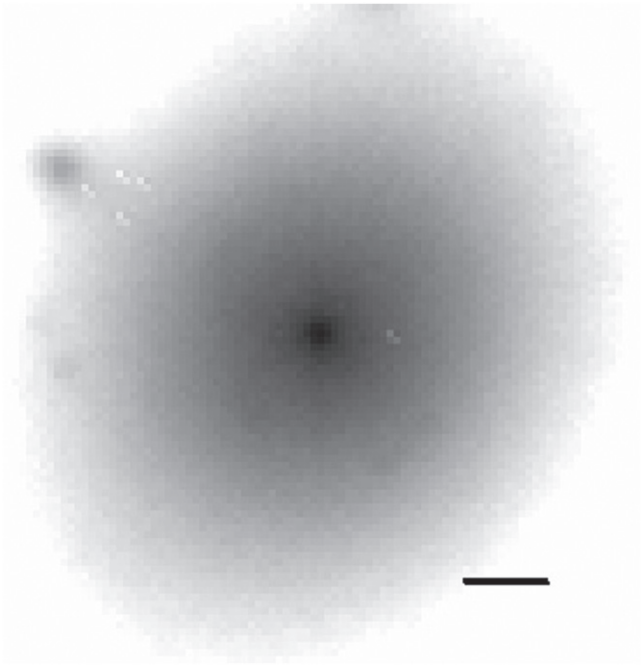

Figure 3. Zoom of the Gemini-GMOS image of the center of Abell 85 showing a clear nuclear emission that is seen on the surface brightness profile as a clear bump in the central kiloparsec, see the top panel of Figure 2. The scale bar on the lower right represents a length of 2 kpc. This image was created using a logarithmic scale.

4. COMPARISON WITH RECENT WORK

López-Cruz et al. (2014) use the Nuker model to fit the surface brightness profile of the BCG of Abell 85, derived with data taken by the KPNO 0.9 m telescope and a seeing of 1.″67. These data are not publicy available, but were given to us by O. López-Cruz.

As shown in the top panel of Figure 2 and in Figure 3, the new Gemini data reveals the presence of nuclear emission. This central and distinct feature is completely absent from the data presented by López-Cruz et al. (2014). In fact, the surface brightness profile presented by the authors above is featureless within the inner 20 kpc of the center of the galaxy.

Using *HST* data, Côté et al. (2006) clearly demonstrate that ground-based data with poor seeing underestimates the presence of nucleii in nearby elliptical galaxies.

The Gemini data shows that from ∼6 kpc inward, the extrapolation of the surface brightness profile results in a light excess, not a light deficit, as one might believe is the case when looking at the lower quality KPNO data. The above is true regardless of the model chosen to fit the surface brightness profile of the galaxy. It should be noted that the surface brightness profiles shown in Figure 2 were derived using data that received no additional processing beyond basic data reduction.

In their analysis of the CFHT data, Bonfini et al. (2015) detect a "tiny bump" in the light profile within the inner 0.″5. Indeed, their core-Sérsic model fits a light excess rather than a light deficit within the inner 0.″5.

At the faint end of the profile, shown in the bottom panel of Figure 2, the KPNO data becomes noisy beyond ∼40 kpc from the center of the galaxy. Similar noise levels are only present in the Gemini data at ∼120 kpc.

5. NUCLEAR EMISSION AND NUCLEAR VARIABILITY

The presence of a clear light excess within the innermost kiloparsec of the BCG of Abell 85 prompts us to discuss its physical origin. One might attribute this nuclear emission to the presence of an active galactic nucleus (AGN) given that BCGs are more likely to host a radio-loud AGN than other galaxies of similar mass (Best et al. 2007). The detection of X-ray emission co-spatial with the galaxy core can be candidly thought to be proof of the existence of an AGN. The picture for Abell 85 is more complex. In fact, Sivakoff et al. (2008) exclude the BCG from a census of active galactic nuclei in Abell 85 given that its position also corresponds, within a few arcseconds, to the peak X-ray emission of the intracluster medium.

AGNs also have distinctive radio emission and Abell 85 has been observed in the radio (Bagchi et al. 1998; Slee et al. 2001; Schenck et al. 2014). Based on the morphology of the radio emission and its spectrum, the above authors do not find evidence of strong AGN activity for the BCG of Abell 85. The radio maps of Abell 85 do not show jets or lobes, which are the clear signatures of strong and current AGN activity. On the contrary, those radio maps are consistent with the presence of radio relics from shocked gas or from a dead radio galaxy, the latter not obviously cospacial with the BCG (Schenck et al. 2014).

We measured the flux difference in the core of the BCG between the CFHT and Gemini images. These images were taken about six years apart: 2008 September (CFHT) and 2014 November (Gemini). Fluxes were measured within an aperture of 1.″5 for each detector. This is the aperture at which the integrated magnitudes of a point source converge for both detectors. We find $\Delta\mathrm{mag} = 0.10 \pm 0.04$, that is, the nucleus of the BCG has become brighter by 0.10 mag during the last six years. This type of optical variability is suggestive of the presence of an AGN in the core of the BCG. It is known that all AGNs vary in short timescales (e.g., Ulrich et al. 1997). We should note that we also measure the flux difference in the core of a dozen random galaxies common to both images and find no difference above the uncertainty level of 0.02 mag.

The variability within the core of the BCG of Abell 85, discussed above, hints to the presence of an AGN but can also be of stellar origin particularly in a dense nuclear stellar structure. Variability is indeed a defining property of AGNs that is often used for their discovery. For instance, Cohen et al. (2006) search for variable galaxies in the Hubble Ultra Deep Field to investigate the presence of AGN and find 45 solid candidates. Those AGN candidates show characteristic variability of Δmag ∼0.01–0.8 mag. On the other hand, dense star clusters are the favorite crash sites for binary stars, cataclysmic variables, and classical novae among other stellar exotica (Knigge et al. 2002). Classical novae have been found in extragalactic globular clusters and their erupting luminosity is comparable to their entire host (Shara et al. 2004).

We find that the core of the Abell 85 BCG is resolved with a FWHM of about 0.″85, that is, about 50% larger than the FWHM of a stellar point-spread function. At the distance of Abell 85, the physical size of the central component is thus ∼0.9 kpc. This central nuclear component, within the first arcsecond, can be easily modeled as a Gaussian function with an integrated magnitude of $m_r = 22.37$ mag.

The resolved stellar structure in the core of the Abell 85 BCG has a physical size that is too large when compared to nuclear star clusters. Indeed, nuclear star cluster sizes are of the

Table 1
Fits to the Surface Brightness Profile of the BCG of Abell 85

Nuker Fits										
μ_b (mag/″^{2})	r_b (″)	r_b (kpc)	α	β	γ	r_γ (kpc)	Seeing (″)	χ^2	Telescope	References
(1)	(2)	(3)	(4)	(5)	(6)	(7)	(8)	(9)	(10)	(11)
21.78	17.21	18.48	1.24	3.33	0.0	4.57	1.67	...	KPNO 0.9 m	López-Cruz et al.
22.32	19.09	20.50	1.22	3.62	0.0	4.57	0.74	...	CFHT 3.5 m	López-Cruz et al.
21.05	10.70	11.56	1.90	2.29	0.14	5.02	0.56	116	Gemini 8 m	This work
Double Sérsic Fit										
μ_1 (mag/″^{2})	r_{e1} (″)	r_{e1} (kpc)	$1/n_1$	μ_2 (mag/″^{2})	r_{e2} (″)	r_{e2} (kpc)	$1/n_2$	χ^2	Telescope	References
(1)	(2)	(3)	(4)	(5)	(6)	(7)	(8)	(9)	(10)	(11)
21.71	14.59	15.68	0.933	24.87	70.79	76.10	0.839	47	Gemini 8 m	This work
Single Sérsic Fit										
μ_1 (mag/″^{2})	r_{e1} (″)	r_{e1} (kpc)	$1/n_1$	...	...	...	...	χ^2	Telescope	References
(1)	(2)	(3)	(4)	(5)	(6)	(7)	(8)	(9)	(10)	(11)
23.24	342.3	368.0	0.13	...	...	...	...	117	Gemini 8 m	This work

Note. Nuker model fits—column (1): surface brightness μ_b; column (2): break radius r_b in arcseconds; column (3): break radius r_b in kiloparsecs; column (4): α power radius at r_b; column (5): β; column (6): γ; column (7): cusp radius r_γ in kiloparsecs; column (8): seeing in arcseconds; column (9): goodness of fit; column (10): telescope in use; column (11): reference. Double and single Sérsic model fits—columns (1) and (5): central surface brightness; columns (2) and (6): effective radius in arcseconds; columns (3) and (7): effective radius in kiloparsecs; columns (4) and (8): inverse of the Sérsic index n; column (9): goodness of fit; column (10): telescope; column (11): reference.

order of a few parsecs (e.g., ∼3 pc; Böker 2010). Also, the largest nuclear structure found by Côté et al. (2006) in their survey of the Virgo Cluster has an effective radius of 62 pc.

Based on its size, a Nuclear Stellar Disk (NSD) is a more compatible candidate for the origin of the nuclear emission of the Abell 85 BCG. For instance, Ledo et al. (2010) compile a census of nuclear stellar disks in early-type galaxies. Several of these NSDs have sizes of a few hundred parsecs with two of them having sizes larger than 1 kpc. If the central structure of Abell 85 is indeed a Nuclear Stellar Disk it would be among the largest reported so far. To give more context, we remark that the catalog of Ledo et al. (2010) is limited to galaxies within 108 Mpc while Abell 85 is at more than twice this distance. Also, the Abell 85 BCG is brigther than the sample studied by Ledo et al. (2010).

Laine et al. (2003) study a sample of BCGs with luminosities and distances similar to those of Abell 85 and find the presence of two nuclear stellar disks (Abell 261 and Abell 1142). Laine et al. (2003) also found an additional seven BCGs with point-like nucleii that exhibit similar morphology to the Abell 85 BCG.

With the current data, we favor a Nuclear Stellar Disk as the physical explanation for the nuclear structure present in the core of the Abell 85 BCG. The nuclear variability we measure is, however, more likely associated with an AGN. Additional data points are needed in order to build a better sampled light curve and unambiguously identify the origin of the variability.

6. FITS TO THE SURFACE BRIGHTNESS PROFILE USING THE NEW GEMINI DATA

Different models used to fit the radial surface brightness profile of galaxies can be found in the literature. Commonly used analytical functions are the Sérsic (1968) profile, which is a generalization of the de Vaucouleurs (1948) and exponential profiles, the Moffat (1969) profile, and the Gaussian profile. Models that use additional parameters to account for the parametrization of galaxy cores are a blend of two power laws (Ferrarese et al. 1994), the Nuker model (Lauer et al. 1995), and the core-Sérsic profile (Graham et al. 2003). The King (1966) model is commonly used to fit the radial light profile of globular clusters and small galaxies.

In this section, the results of fitting different analytical models to the new Gemini data are presented. The results of our best fits and the fits of López-Cruz et al. (2014) are shown in Table 1. The fits below are applied to the deconvolved image. The fits are carried out to a galactocentric distance of 115 kpc, that is, where the standard deviation of the sky (∼0.3 mag) equals the uncertainty on the galaxy surface brightness.

6.1. de Vaucouleurs

Schombert (1987) showed that a de Vaucouleurs (1948) model fails to properly fit the surface brightness profile of the Abell 85 BCG. A de Vaucouleurs fit for this galaxy overestimates the flux at the center while it underestimates the flux in the outskirts. Schombert (1987), also showed that this result was also true for several other BCGs.

6.2. Single Sérsic

We fit a single Sérsic profile to the new Gemini data. For clarity, we define the Sérsic profile in its canonical form R^β, where the concentration parameter $\beta = 1/n$ is the inverse of

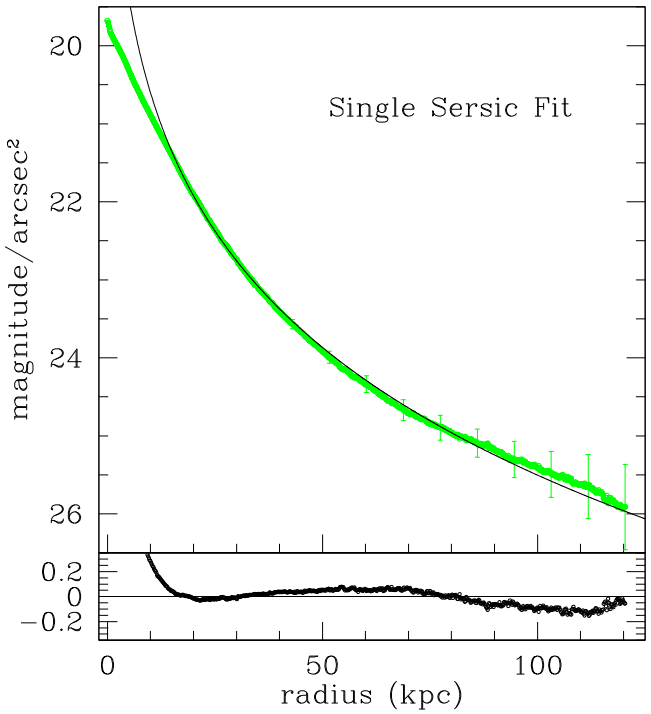

Figure 4. Single Sérsic fit to the new Gemini data (green). A single Sérsic profile (solid black line) provides a good fit to the main body of the surface brightness profile, but fails to model the data within the inner ∼18 kpc. Residuals are shown in the bottom panel.

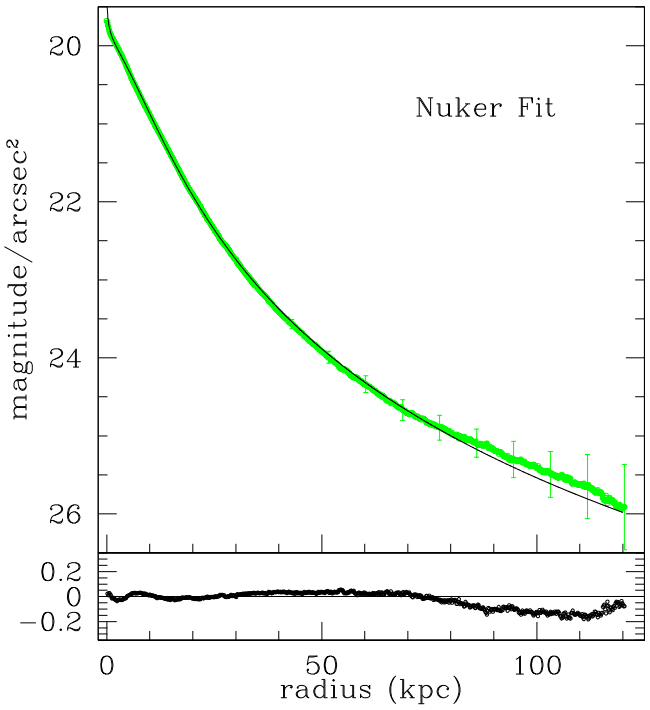

Figure 5. Best Nuker model fit (solid line) to the new Gemini data (green). Residuals are shown in the bottom panel.

the Sérsic index (Sérsic 1968):

$$I(r) = I_e \exp\left\{-b_n\left[\left(\frac{r}{r_e}\right)^{\beta} - 1\right]\right\}. \quad (1)$$

In this equation I_e is the intensity at $r = r_e$ at the effective radius. The values for b_n can be calculated using $b_n \sim 2n - 0.33$ (Caon et al. 1993).

The best fit of the Sérsic model to the Gemini data is shown in Figure 4. We find that a single Sérsic provides a good fit to the data only over a limited section of the surface brightness profile. Model and data diverge at small radii, that is, for radii below ∼18 kpc.

The numerical parameters of the best fit using a single Sérsic model, such as an exceedingly large effective radius, expose the fact that this model does not provide a good physical representation of the overall surface brightness profile.

Studying a large sample of elliptical galaxies, Kormendy et al. (2009) also find that a single Sérsic profile is a good fit to the main section of the radial profile, while the model deviates from the data at small radii. Similarly, Lasker et al. (2014) need to include additional components beyond a single Sérsic profile when fitting the surface brightness profile of 35 nearby galaxies. Additional models correspond to additional physical components such as bars, nuclei, inner disks, and envelopes.

6.3. Nuker Model

We also fit a Nuker model to the Gemini data and present the results in Figure 5. Numerical parameters are given in Table 1. Interestingly, we find an even larger cusp radius, $r_\gamma = 5.02$ kpc than the one found by López-Cruz et al. (2014). We find, however, a break radius of $r_b = 11.6$ kpc, almost half the value of López-Cruz et al. (2014).

An important caveat to fitting a Nuker model to this galaxy is the fact that it does not actually have a flat evacuated core and the Nuker model does not identify the presence of the nuclear component. The existence of this distinct nuclear component naturally changes the results given by the Nuker model fit, as shown above. Also, it has been proven that the Nuker model is dependent on the radial extent of the fit (Graham et al. 2003). Moreover, the Nuker model was never intended to fit the entire surface brightness profile, but the central region of any given galaxy—see the recent work of Bonfini et al. (2015) and references therein.

The Nuker model used by López-Cruz et al. (2014) underestimates their data beyond ∼20 kpc. The failure of the Nuker profile at large radii prompts López-Cruz et al. (2014) to fit a de Vaucouleurs profile (i.e., Sérsic profile with $n = 4$). It should be noted that the de Vaucouleurs profile used by López-Cruz et al. (2014) overestimates their data in the outskirts of the galaxy.

6.4. Core-Sérsic

In a recent work, Bonfini et al. (2015) carry out a detailed re-analysis of the CFHT data of the Abell 85 BCG focusing on fitting the core-Sérsic model. Bonfini et al. (2015) find that the Abell 85 BCG does not have a depleted core because the light profile does not show a light deficit when fitted with the core-Sérsic model. In fact, these authors find that the Abell 85 BCG is not well adjusted by a core-Sérsic due to a light excess in its central surface brightness profile. Bonfini et al. (2015) find that the Abell 85 BCG is a coreless galaxy whose surface brightness profile is best fit by an inner Sérsic profile and an outer exponential halo.

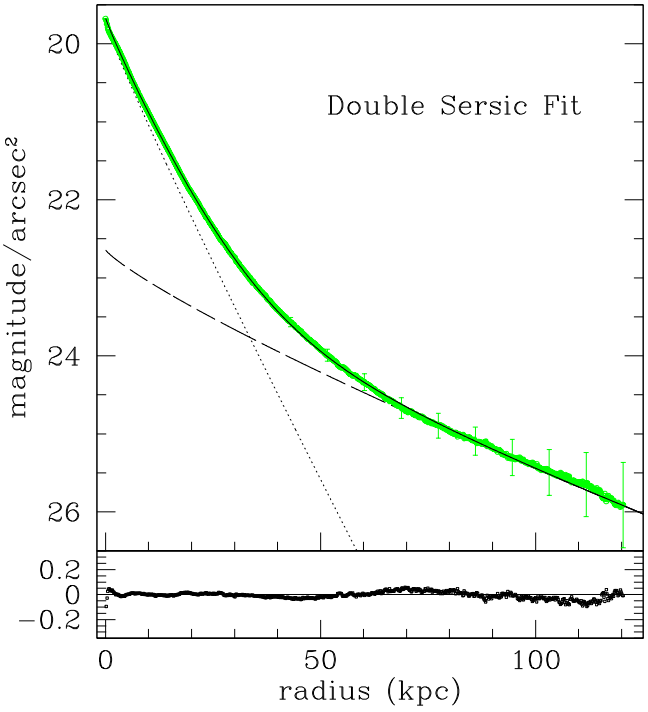

Figure 6. Double Sérsic fit to the new Gemini data (green). Dashed and dotted lines represent the two inner and outer Sérsic components. The solid line, indistinguishable from the data, is the sum of the two components. Residuals are shown in the bottom panel.

6.5. Double Sérsic

Gonzalez et al. (2003, 2005) and Seigar et al. (2007) showed that two component models are necessary to accurately fit the surface brightness profiles of BCGs. The two components pertain to an inner and outer component. The existence of an outer component reflects the fact that BCGs often have extended envelopes (Schombert 1987). Donzelli et al. (2011) studied the luminosity profiles of 430 BCGs and found that about half of them required a double Sérsic model (Sérsic + exponential). In fact, Donzelli et al. (2011) fit the Abell 85 BCG with an inner Sérsic model and an outer exponential component.

We fit a double Sérsic profile to the Gemini data, and obtain satisfactory results. The values of our best fit are shown in Table 1 and Figure 6. One component has a Sérsic index of $1/n = 0.93$ (dashed line) while the second Sérsic has and index of $1/n = 0.84$ (dotted line). The sum of these two components (a solid line) is indistinguishable from the data.

Models that explain the underlying physical mechanisms that create double Sérsic components have been postulated by Cooper et al. (2015). These authors postulate that for BCGs, the double Sérsic profile originates from the superposition of two debris components of different progenitors. The inner profile is associated with relaxed accreted components while the outer profile corresponds with unrelaxed accreted debris (Cooper et al. 2015).

The best fit to the surface brightness of this galaxy is given by a double Sérsic model. Values for the goodness of fit (χ^2) are presented in Table 1 and a residual image is shown on Figure 7. We should note that the χ^2 value given for the single Sérsic fit pertains to a fit between 20 and 115 kpc, a fit over the whole range of the data would yield $\chi^2 = 2750$.

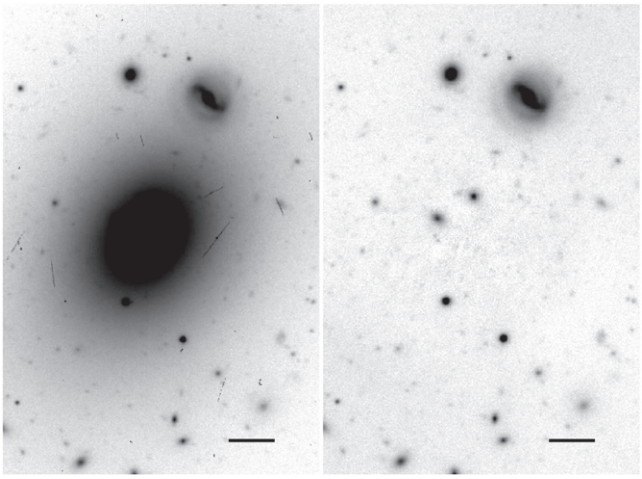

Figure 7. Original image (left) and residual after subtraction of the double Sérsic model (right). No visible structure is left on the residual image. The scale bar on the lower right represents a length of 10 kpc. This image was made using a logarithmic display.

7. DOES THE ABELL 85 BCG HOST THE MOST MASSIVE BLACK HOLE IN THE UNIVERSE?

Based on the analysis of new Gemini data presented above, we conclude that the Abell 85 BCG (Holm 15A) is a nucleated, coreless galaxy. That is, it does not have an exceptionally large core due to a light deficit in its central region (López-Cruz et al. 2014). Our results thus nullify the existence of a supermassive black hole based solely on the presence of a depleted core, which this galaxy, in fact, does not have.

By fitting the Nuker model to the surface brightness profile, we find a large cusp and break radius. We refrain from interpreting the cusp and break radius as representative of an evacuated core created by the scouring action of a binary black hole. A large cusp radius, derived from the Nuker model, does not necessarily imply a downward bend of the inner light profile.

Recently, Bonfini et al. (2015) pointed out that the presence of a singular point in the surface brightness profile of any given galaxy does not imply the presence of a depleted core. In the words of Bonfini et al. (2015), most galaxies have particular values for the negative logarithmic slope of the intensity profile, but this is not a sufficient condition for the existence of a depleted core.

Moreover, the central brightness profile of the Abell 85 BCG is indeed different from the flat, or even decreasing surface brightness profile of, for instance, the BCG of Abell 2261 (Postman et al. 2012). The presence of a nuclear structure is difficult to reconcile with a core of ∼5 kpc where other stars within that core are ejected.

The authors would like to thank the referee for a detailed and constructive report that helped us improve this paper. We are grateful to Nancy Levenson, Gemini Head of Science, for granting us Director Discretionary Time to carry out these observations under program GS-2014B-DD-6. We also thank Gemini observer Mischa Schirmer, and Gemini visiting astronomer Ricardo de Marco for obtaining the data. The CFHT data was kindly shared with us by Melissa Graham and David Sand, likewise, the KPNO data was made available to us by Omar Lopez-Cruz. This research has made use of the NASA

Astrophysics Data System Bibliographic services (ADS) and Google. This work was supported by a grant from SECYT-UNC, Argentina.

Based on observations obtained at the Gemini Observatory, which is operated by the Association of Universities for Research in Astronomy, Inc., under a cooperative agreement with the NSF on behalf of the Gemini partnership: the National Science Foundation (United States), the National Research Council (Canada), CONICYT (Chile), the Australian Research Council (Australia), Ministério da Ciência, Tecnologia e Inovação (Brazil) and Ministerio de Ciencia, Tecnología e Innovación Productiva (Argentina).

REFERENCES

Bagchi, J., Pislar, V., & Lima Neto, G. B. 1998, MNRAS, 296, L23
Begelman, M. C., Blandford, R. D., & Rees, M. J. 1980, Natur, 287, 307
Best, P. N., von der Linden, A., Kauffman, G., Heckman, T. M., & Kaiser, C. R. 2007, MNRAS, 379, 894
Böker, T. 2010, in Proc. IAU Symp. 266, Star Clusters: Basic Building Blocks throughout Time and Space (Cambridge: Cambridge Univ. Press), 58
Bonfini, P., Dullo, B. T., & Graham, A. W. 2015, ApJ, 807, 136
Caon, N., Capaccioli, M., & D'Onofrio, M. 1993, MNRAS, 265, 1013
Cohen, S. H., et al. 2006, ApJ, 639, 731
Cooper, A. P., Gao, L., Guo, Q., et al. 2015, MNRAS, 451, 2703
Côté, P., et al. 2006, ApJS, 165, 57
De Lucia, G., & Blaizot, J. 2007, MNRAS, 375, 2
de Vaucouleurs, G. 1948, AnAp, 11, 247
Donzelli, C. J., Muriel, H., & Madrid, J. P. 2011, ApJS, 195, 15
Durret, F., Felenbok, P., Lobo, C., & Slezak, E. 1998, A&AS, 129, 281
Durret, F., Lima Neto, G. B., & Forman, W. 2005, A&A, 432, 809
Faber, S., et al. 1997, AJ, 114, 1771
Ferrarese, L., et al. 2006, ApJS, 164, 334
Ferrarese, L., van den Bosch, F. C., Ford, H. C., Jaffe, W., & O'Connell, R. W. 1994, AJ, 108, 1598
Fogarty, L. M. R., et al. 2014, MNRAS, 443, 485
Gonzalez, A. H., Zabludoff, A. I., & Zaritsky, D. 2003, Ap&SS, 285, 67
Gonzalez, A. H., Zabludoff, A. I., & Zaritsky, D. 2005, ApJ, 618, 195
Graham, A. W., Erwin, P., Trujillo, I., & Asensio Ramos, A. 2003, AJ, 125, 2951
Ichinohe, Y., et al. 2005, MNRAS, 448, 2971
Jedrzejewski, R. 1987, MNRAS, 226, 747
Jones, C., & Forman, W. 1984, ApJ, 276, 38
Kempner, J. C., Sarazin, C. L., & Ricker, P. M. 2002, ApJ, 579, 236
King, I. R. 1966, AJ, 71, 64
Knigge, C., Zurek, D. R., Shara, M. M., & Long, K. S. 2002, ApJ, 579, 752
Kormendy, J., Fisher, D. B., Cornell, M. E., & Bender, R. 2009, ApJS, 182, 216
Kormendy, J., & Ho, L. C. 2013, ARA&A, 51, 511
Laine, S., et al. 2003, AJ, 126, 2717
Lasker, R., Ferrarese, L., & van de Ven, G. 2014, ApJ, 780, 69
Lauer, T., et al. 1995, AJ, 110, 2622
Ledo, H. R., Sarzi, M., Dotti, M., Khochfar, S., & Morelli, L. 2010, MNRAS, 407, 969
Lima Neto, G. B., Pislar, V., & Bagchi, J. 2001, A&A, 368, 440
López-Cruz, O., et al. 2014, ApJL, 795, L31
Lucy, L. B. 1974, AJ, 79, 745
Markevitch, M., Forman, W. R., Sarazin, C. L., & Vikhlinin, A. 1998, ApJ, 503, 77
Milosavljević, M., & Merritt, D. 2001, ApJ, 563, 34
Moffat, A. F. J. 1969, A&A, 3, 455
Postman, M., et al. 2012, ApJ, 756, 159
Richardson, W. H. 1972, JOSA, 62, 55
Sand, D. J., et al. 2011, ApJ, 729, 142
Schenck, D. E., Datta, A., Burns, J. O., & Skillman, S. 2014, AJ, 148, 23
Schombert, J. M. 1987, ApJS, 64, 643
Seigar, M. S., Graham, A. W., & Jerjen, H. 2007, MNRAS, 378, 1575
Sérsic, J. L. 1968, Atlas de Galaxias Australes (Córdoba: Observatorio Astronómico)
Shara, M. M., Zurek, D. R., Baltz, E. A., Lauer, T. R., & Silk, J. 2004, ApJL, 605, L117
Sivakoff, G. R., Martini, P., Zabludoff, A. I., Nelson, D. D., & Mulchaey, J. S. 2008, ApJ, 682, 803
Slee, O. B., Roy, A. L., Murgia, M., Andernach, H., & Ehle, M. 2001, AJ, 122, 1172
Ulrich, M.-E., Maraschi, L., & Urry, C. M. 1997, ARA&A, 35, 445
White, S. D. M., & Rees, M. J. 1978, MNRAS, 183, 341